$YCa_3(MnO)_3(BO_3)_4$: A manganese borate containing ferromagnetic chains on a kagomé lattice

R. K. Li[1,2] and C. Greaves[1]

[1]*School of Chemical Sciences, The University of Birmingham, Edgbaston, Birmingham B15 2TT, United Kingdom*

[2]*Beijing Center of Crystal Research and Development, Technical Institute of Physics and Chemistry, Chinese Academy of Sciences, Beijing 100080, China*

(Received 20 May 2003; revised manuscript received 13 August 2003; published 13 November 2003)

A new borate compound $YCa_3(MnO)_3(BO_3)_4$ derived from the mineral gaudefroyite was prepared. It adopts a hexagonal space group $P6_3/m$ with cell parameters of $a=10.5726(5)$ Å and $c=5.8576(3)$ Å. Structural studies by x-ray and neutron powder diffraction (NPD) revealed that it is composed of edge-sharing chains of MnO_6 octahedra along *c*, the chains being interconnected by triangular BO_3 groups to form a kagomé lattice in the *ab* plane. Both magnetic measurements and low-temperature NPD showed that the Mn ions within a given MnO chain are ferromagnetically coupled and, below 7.5 K, the magnetic moments of the chains order to give a normal $q=0$ structure of the kagomé lattice.

DOI: 10.1103/PhysRevB.68.172403 PACS number(s): 75.30.Cr, 61.12.Ld, 75.25.+z, 75.50.Ee

When three magnetic ions sit at the vertices of a triangle and experience antiferromagnetic (AFM) interactions, antiparallel alignment of all neighboring spins cannot be simultaneously fulfilled; the spins are therefore frustrated. Studies of the statistical properties of geometrically frustrated magnetic compounds have stimulated much attention owing to their relation to the broad physical behavior of systems ranging from neural networks, Josephson junction arrays, and negative thermoexpansion materials to ^{3}He absorption on graphite.[1–4] Tiling the triangles in two dimensions by edge or vertex sharing can result in triangular or kagomé lattices. Mean-field theory predicted that no magnetic order can be obtained on a kagomé lattice even at $T=0$ K, owing to its unusually large number of degenerate ground states.[5] However, long-range order can be established through next-nearest-neighbor interactions or by thermal fluctuation.[6,7] Especially, the latter mechanism, known to be order by disorder,[8] favors the so-called $\sqrt{3}\times\sqrt{3}$ magnetic structure. Few real materials can be modeled as a kagomé lattice; examples include $SrCr_8Ga_4O_{19}$, $Ba_2Sn_2Ga_3ZnCr_7O_{22}$, and jarosites $[KM_3(SO_4)_2(OH)_6$, $M=Fe^{3+}$, Cr^{3+}, $V^{3+}]$.[9–11] The problem of all the above compounds is their nonstoichiometry, which hinders the reproducibility of physical property measurements. In jarosites, maximum magnetic ion occupancy can only be achieved up to 98%, while in $SrCr_8Ga_4O_{19}$ and $Ba_2Sn_2Ga_3ZnCr_7O_{22}$ mixing of different ions at the Cr sites is sometimes unavoidable because of the coexistence of many ions of similar size and chemical properties. Furthermore, in $SrCr_8Ga_4O_{19}$, the existence of an extra double layer of a triangular lattice further complicates the interpretation of its magnetic properties. At low temperature, magnetic order has been found in some samples of the above compounds, especially those with a large concentration of defects at the magnetic sites, while those with a perfect magnetic lattice tend to show spin-glass behavior.

Transition-metal borates can be a natural source of new triangular magnets, owing to the occurrence of planar BO_3 triangular groups. When magnetic ions are joined by the BO_3 groups, they often form a perfect triangular lattice, as demonstrated by $LiMnBO_3$.[12] The compound studied here derives from the mineral gaudefroyite $Ca_4(MnO)_3(BO_3)_3CO_3$ by replacing the isolated CO_3^{2-} group with a BO_3^{3-} group and achieving charge balance by simultaneously substituting one Ca^{2+} with Y^{3+}. Gaudefroyite has been reported as having a hexagonal lattice with space group $P6_3$ or $P6_3/m$ and unit cell dimensions $a=10.589$ Å and $c=5.891$ Å.[13,14] Its structure is composed of MnO_6 octahedra, which are edge shared to produce chains [Fig. 1(a)] along the *c* direction and these chains form a kagomé lattice in the *ab* plane [Fig. 1(b)]. In order to study the magnetic behavior of the MnO chains on the kagomé lattice and avoid the decomposition of the CO_3 group when preparing gaudefroyite, we investigated the synthesis of the new compound $YCa_3(MnO)_3(BO_3)_4$. Both x-ray and neutron powder diffraction (NPD) proved that it is isostructural to gaudefroyite.

Samples of $YCa_3(MnO)_3(BO_3)_4$ were prepared from $CaCO_3$, Y_2O_3, Mn_2O_3, and ^{11}B isotope enriched boric acid by solid-state reaction at 1000–1100 °C. Time-of-flight NPD data were collected at GEM (ISIS, RAL, Oxford, UK). Magnetic measurements were performed with a Quantum Design PPMS magnetometer. Structure refinements were carried out using the NPD data and the GSAS package.[15] In all the refinements, data collected from both bank 2 ($2\theta=154.46°$) and bank 5 ($2\theta=17.95°$) were used simultaneously.

Structure refinements of the room-temperature NPD data were performed with space groups $P6_3$ and $P6_3/m$ separately. The use of space group $P6_3$ resulted in large estimated standard deviations (ESD's) in the *z* coordinates of atoms with variable *z* parameters. This suggests the presence of a pseudo mirror plane perpendicular to the *c* axis,[14] and subsequent refinements in $P6_3/m$ gave much smaller ESD's and smaller agreement indices ($R_{wp}=4.53$, $\chi^2=1.933$ for $P6_3/m$ vs $R_{wp}=5.17$, $\chi^2=2.499$ for $P6_3$). The final refinement was therefore performed with space group $P6_3/m$ and a total of 88 variables. In the hexagonal tunnels, a statistical occupation of the BO_3 groups at above and below the mirror plane is found, as has also been suggested for CO_3 in the single-crystal study on gaudefroyite.[14] The refined lattice constants are $a=10.5726(5)$ Å and $c=5.8576(3)$ Å, slightly smaller than its mineral analog, since it contains the smaller

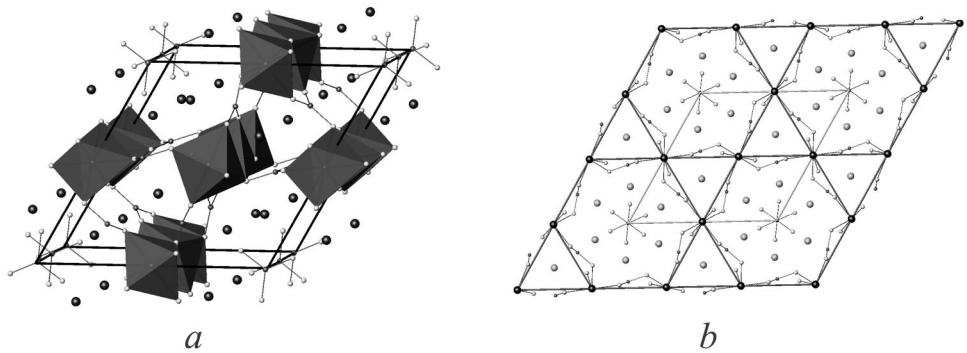

FIG. 1. Crystal structure of $YCa_3(MnO)_3(BO_3)_4$ (a) showing the MnO_6 chains along c in the unit cell and (b), showing the magnetic Mn^{3+} ions arranged into a perfect kagomé lattice in the ab plane. Small isolated balls are the Ca/Y atoms.

Y^{3+} ion. The refined structural parameters are listed in Table I. The major difference between the present compound and gaudefroyite centers in the tunnels within the kagomé net of MnO chains. The hexagonal tunnel now contains isolated BO_3^{3-} oxoanions instead of CO_3^{2-}, and a mixture of Ca^{2+}/Y^{3+} ions instead of purely Ca^{2+} occupies the sites in both the trigonal and hexagonal tunnels. It is also worth noting that the Y^{3+} ion seems to prefer to reside in the trigonal tunnel (occupancy $n\sim0.5$) rather than the hexagonal one ($n\sim0.16$). This is consistent with size effects since the bond valence sum[16] of Ca is 2.0+in the hexagonal tunnel while in the trigonal tunnel it is 2.2+.

Magnetic susceptibility in low fields [Fig. 2(a), dc, $H=1000$ G, and ac, $H=5$ G] shows a sharp peak at 7.5 K, indicating AFM ordering below this temperature. Above 70 K, it can be well fitted with the Curie-Weiss law, $\chi=C/(T-\theta)$, with $\theta=27.2(3)$ K and $\mu_{\rm eff}=5.15(1)\mu_B/(\rm Mn)$, where $C=Ng^2\mu_{\rm eff}^2/3k$. The ferromagnetic (FM) behavior ($\theta>0$) above the AFM transition can be attributed to the Mn-O-Mn superexchange along the chains since it is the dominant interaction in the present compound (with nearest Mn-Mn distance of 2.9288 Å along the chain versus 5.2863 Å in the ab plane). The effective moment derived here is slightly larger than that expected for a high-spin (HS) Mn^{3+} (d^4, HS, $\mu_{\rm eff}=4.9\mu_B$) ion, which is sometimes observed in frustrated systems like spin glasses[17] and may be attributed to competing FM (within chains) and AFM (in-plane) interactions at low temperature. Magnetizations around the transition temperature were measured up to 7 T. Well above the transition, at 50 K, typical paramagnetic behavior was observed (with $m\propto H$) as shown in Fig. 2(b). At temperatures close to the transition, FM behavior is observed and nearly full alignment of the magnetic moments could be achieved; e.g., a saturated moment of $3.83\mu_B$ was observed at 2 K and 7 T, very close to ideal Mn^{3+} value of $4\mu_B$. Both the slopes of magnetization data against field and susceptibilities under different fields [Fig. 2(b), inset] show that the susceptibility peak at 7.5 K disappears at fields greater than 5000 G. The fact that AFM order can be suppressed in such a small field highlights the frustrated nature of the AFM interaction in the ab plane.[17]

The only noticeable difference between low- and room-temperature NPD patterns (Fig. 3) is that the (010) peak intensity grows significantly below the transition temperature 7.5 K. Several magnetic structure models were tested; a model with a normal $q=0$ structure [shown in Fig. 4(b)] for the kagomé lattice in the ab plane and ferromagnetic intrachain coupling along c agrees best with the observed NPD pattern and is also consistent with the observation of a dominant FM interaction above 70 K followed by AFM ordering

TABLE I. Refined structural data of $YCa_3(MnO)_3(BO_3)_4$ at room temperature and 2 K.

		RT					2 K [a]			
Atoms	Sites	x	y	z	U_{iso}	n	x	y	z	U_{iso}
Ca/Y1	$2c$	$\frac{1}{3}$	$\frac{2}{3}$	$\frac{1}{4}$	0.0060(7)	0.49/0.51(2)	$\frac{1}{3}$	$\frac{2}{3}$	$\frac{1}{4}$	0.0026(3)
Ca/Y2	$6h$	0.1223(3)	0.8375(3)	$\frac{1}{4}$	0.0066(5)	0.837/0.163(5)	0.1224(2)	0.8372(2)	$\frac{1}{4}$	0.0021(2)
Mn	$6g$	$\frac{1}{2}$	0	0	0.0013(4)	1	$\frac{1}{2}$	0	0	0.0001 [b]
B1	$6h$	0.2200(2)	0.7686(2)	$\frac{3}{4}$	0.0042(3)	1	0.2217(1)	0.7697(1)	$\frac{3}{4}$	0.0016(1)
B2	$4e$	0	0	0.0749(6)	0.0036(7)	$\frac{1}{2}$	0	0	0.0756(5)	0.0020(5)
O1	$6h$	0.0937(2)	0.4706(2)	$\frac{1}{4}$	0.0044(4)	1	0.0929(2)	0.4695(2)	$\frac{1}{4}$	0.0027(2)
O2	$6h$	0.3209(2)	0.9171(2)	$\frac{3}{4}$	0.0052(4)	1	0.3218(2)	0.9168(2)	$\frac{3}{4}$	0.0017(1)
O3	$12i$	0.3035(2)	0.4761(2)	0.5429(2)	0.0072(3)	1	0.3029(1)	0.4762(1)	0.5426(2)	0.0032(1)
O4	$12i$	0.0590(3)	0.9098(3)	0.5845(5)	0.0100(6)	$\frac{1}{2}$	0.0594(2)	0.9095(2)	0.5829(4)	0.0057(4)
Space group:	$P6_3/m$	$a=10.5726(5)$ Å, $c=5.8576(3)$ Å					$a=10.5555(1)$ Å, $c=5.8531(1)$ Å			
		$R_{wp}=4.53\%$, $\chi^2=1.933$					$R_{wp}=7.49\%$, $\chi^2=1.670$			

[a]Magnetic space group $P6_3'$, $a=a_{\rm N}$, $c=c_{\rm N}$, $m_x^{Mn}=1.74(1)\mu_B$.
[b]Fixed.

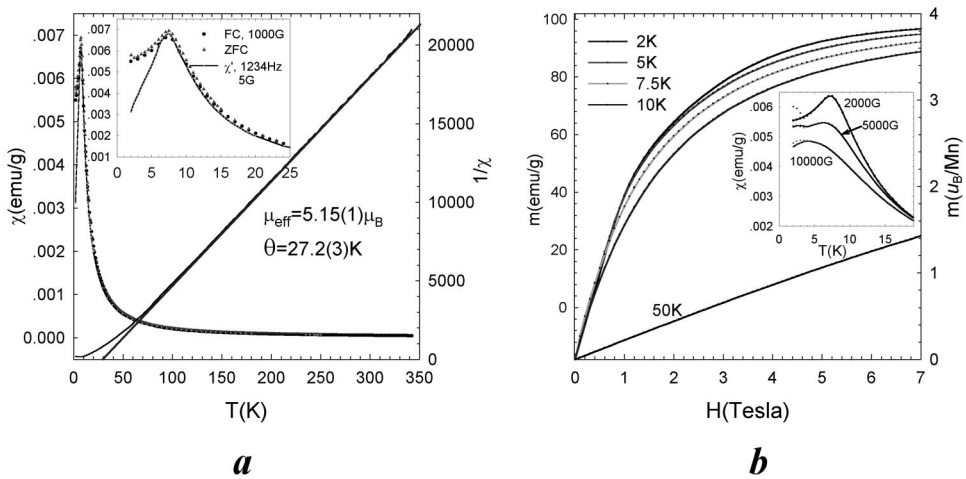

FIG. 2. Magnetic susceptibility (a) and low-temperature magnetization (b) of $YCa_3(MnO)_3(BO_3)_4$. The inset in (b) shows magnetic susceptibilities under different magnetic fields; dots are field-cooled data and lines are zero-field-cooled data.

at 7.5 K from magnetic measurements. The ordered magnetic moment was found to be $1.74(1)\mu_B$ from the refinement of the NPD data at 2 K, much lower than expected for fully ordered Mn^{3+} moment ($4\mu_B$), indicating that a significant fraction of the moments remain paramagnetic or experience only short-range order. Actually, a very broad diffuse scattering maximum in the background was also found below the main magnetic peak at (010), suggesting some kind of short-range order in the *ab* plane. The 120° AFM order among the Mn ions in the *ab* planes is to be expected and was also observed in $LiMnBO_3$. However, it is difficult to explain the observed Mn-Mn ferromagnetic interaction along the chains. Although it is generally believed that 90° metal-oxygen-metal interaction is FM,[18,19] it has been shown[19] that Mn-O-Mn in MnO is AFM and this is also the situation in $LiMnBO_3$. The observation of FM must be linked to a structural peculiarity of the present compound or the presence of Mn^{3+} rather than Mn^{2+}. Figure 4(a) depicts part of the Mn-O-Mn chain and its environment which is important to the magnetic exchange pathways. Due to Jahn-Teller distortion of the Mn^{3+} ion, Mn-O bonds fall into three groups with bond lengths of Mn-O1, 1.879(1) Å; Mn-O2, 2.199(2) Å; and Mn-O3, 1.979(2) Å. There are two near-90° Mn-O-Mn connections along the chains. One is through the shortest bonds with a larger angle Mn-O1-Mn (102.4°) and free from bonding to boron atoms. Because the population of *d* orbitals toward this bond is empty and the angle is close to the transition value ($125° < \alpha_c < 150°$ from Ref. 18, ~97° from Refs. 20 and 21, and 127° from Ref. 22) of superexchange from FM to AFM, any residual FM interaction strength must be very small through this bond. The second linkage occurs via the longest bonds with smaller angle Mn-O2-Mn (83.5°) and with O2 bonds to B; the *d* orbital of this bond is populated. The coupling between populated Mn-O2-Mn bonds should be FM, but O2 bonding to boron atom further complicates the situation and enhances AFM according to Geertsma and Khomskii;[23] AFM is indeed observed in $LiMnBO_3$. All other direct-direct interactions favor AFM as well. So the MnO chain cannot be FM through the usual superexchange or direct exchange unless some degree of charge fluctuation along the chain takes place: i.e., leading to a double-exchange mechanism,[24] which seems to be also unlikely since resistance measured on a needle crystal showed it is insulating.

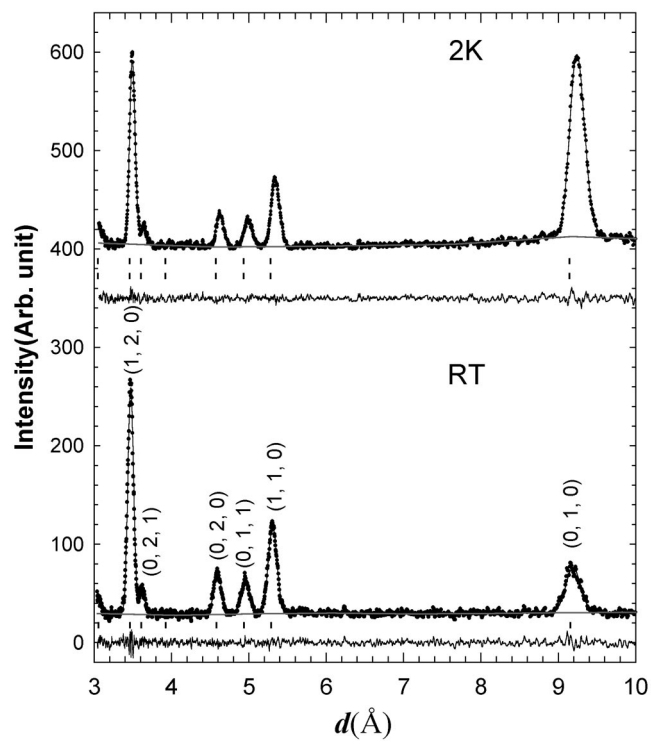

FIG. 3. Neutron diffraction patterns of $YCa_3(MnO)_3(BO_3)_4$ at 2 K and room temperature (only bank-2 data are shown here). The dots are observed data, lines are calculated and difference plots, and vertical marks represent the allowed nuclear and magnetic (2 K only) diffraction peaks. The lines running through the bottoms of the diffraction peaks are the background curve.

Ramirez defined a factor of $f = \theta/T_c$ as an empirical measure of frustration and for the strong geometrically frustrated system $f > 10$.[25] For the present compound, $f = 27.2/7.5 < 4$. However, the applicability of this criterion is questionable because the Weiss constant ($\theta = 27.2$ K) may not even define the three-dimensional θ but only reflect the interaction

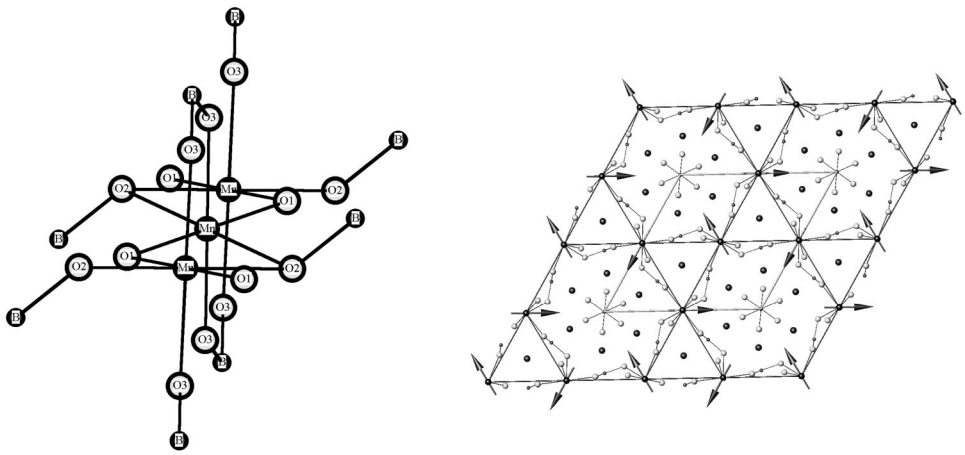

FIG. 4. The environment around the MnO_6 chain (a) and magnetic structure of $YCa_3(MnO)_3(BO_3)_4$ (b). Important bond lengths and angles are Mn-Mn, 2.9288(2) Å; Mn-O1, 1.879(1) Å; Mn-O2, 2.199(2) Å; Mn-O3, 1.979(1) Å; and Mn-O1-Mn, 102.4(1)°, and Mn-O2-Mn, 83.5(1)°, at room temperature.

through the one-dimensional MnO_6 chains. The true value of f must be defined by the ratio of the in-plane AFM interaction and ordering temperature, which could be even smaller because the in-plane interaction is less important than the interaction through the MnO_6 chain. The extremely small value of f found here must reflect magnetic order induced by a large correlation length along the MnO_6 chains at low temperature. It must be pointed out that although it is well established that the site defects enhance magnetic ordering—e.g., in jarosites—we believe that the disorder mechanism from random occupation of Y and Ca ions in the tunnels would have little impact on the magnetic lattice of $YCa_3(MnO)_3(BO_3)_3$, in which the kagomé net is essentially isolated from the cations. In any case, a study of its mineral counterpart gaudefroyite $Ca_4(MnO)_3(BO_3)_3CO_3$ which is free from Y/Ca mixing is clearly very desirable.

We thank EPSRC and the Chinese Academy of Sciences for financial support and E. McCabe and Dr. L. Chapon for their assistance in collecting the NPD data.

[1] A. P. Ramirez, *Handbook of Magnetic Materials* (Elsevier Science B.V., Amsterdam, 2001), Vol. 13, p. 423.
[2] M. F. Collins and O. A. Petrenko, Can. J. Phys. **75**, 605 (1997).
[3] H. Kawamura, J. Phys.: Condens. Matter **10**, 4707 (1998).
[4] J. E. Greedan, J. Mater. Chem. **11**, 37 (2001).
[5] J. N. Reimers, A. J. Berlinsky, and A. C. Shi, Phys. Rev. B **43**, 865 (1991).
[6] A. B. Harris, C. Kallin, and A. J. Berlinsky, Phys. Rev. B **45**, 2899 (1992).
[7] J. N. Reimers and A. Berlinsky, Phys. Rev. B **48**, 9539 (1993).
[8] A. Chubukov, Phys. Rev. Lett. **69**, 832 (1992).
[9] X. Obradors, A. Labarta, A. Isalgué, J. Tejada, J. Rodriguez, and M. Pernet, Solid State Commun. **65**, 189 (1988).
[10] I. S. Hagemann, Q. Huang, X. P. A. Gao, A. P. Ramirez, and R. J. Cava, Phys. Rev. Lett. **86**, 894 (2001).
[11] A. S. Wills, Phys. Rev. B **63**, 064430 (2001), and references therein.
[12] R. K. Li, C. T. Chen, and C. Greaves, Phys. Rev. B **66**, 052405 (2002).
[13] O. V. Yakubovich, M. A. Simonov, and N. V. Belov, Sov. Phys. Crystallogr. **20**, 87 (1975).
[14] C. Hoffmann, T. Armbruster, and M. Kunz, Eur. J. Mineral. **9**, 7 (1997).
[15] A. C. Larson and R. B. von Dreele, *General Structure Analysis System* (Los Alamos National Laboratory, Los Alamos, NM, 1994).
[16] I. Brown and D. Altermatt, Acta Crystallogr., Sect. B: Struct. Sci. **41**, 244 (1985).
[17] J. Mydosh, *Spin Glasses: An Experimental Introduction* (Taylor & Francis, London, 1993), p. 46.
[18] J. Goodenough, *Magnetism and the Chemical Bond* (Interscience, New York, 1963).
[19] J. Kanamori, J. Phys. Chem. Solids **10**, 87 (1959).
[20] van H. Crawford, H. W. Richardson, J. R. Wasson, D. J. Hodgson, and W. E. Hatfield, Inorg. Chem. **15**, 2107 (1976).
[21] Y. Mizuno, T. Tohyama, S. Maekawa, T. Osafune, N. Motoyama, H. Eisaki, and S. Uchida, Phys. Rev. B **57**, 5326 (1998).
[22] M. A. Subramanian, A. P. Ramirez, and W. J. Marshall, Phys. Rev. Lett. **82**, 1558 (1999).
[23] W. Geertsma and D. Khomskii, Phys. Rev. B **54**, 3011 (1996).
[24] C. Zener, Phys. Rev. **81**, 440 (1951); **82**, 403 (1951).
[25] A. P. Ramirez, Annu. Rev. Mater. Sci. **24**, 453 (1994).